Variability of Spectral Estimates of Stress Drop Reconciled by Radiated Energy

Chen Ji*[1,2], Ralph J. Archuleta[1,2], and Yongfei Wang[3]

ABSTRACT

A review of a collection of theoretical source spectral models revealed: (1) Despite the well-known variation in predicting static stress drop $\Delta\sigma_s$ from the seismic moment and corner frequency, all models, especially the three conventional models, suggest that earthquakes radiate about half of the available strain energy into the surrounding medium. This similarity justifies a less model-dependent approach to estimate $\Delta\sigma_s$, though estimates for natural earthquakes rely on apparent seismic radiation efficiency ($= 2\sigma_a/\Delta\sigma_s$; σ_a is apparent stress of an earthquake). (2) When one attempts to use $\Delta\sigma_s$ and spectral models to make predictions, such as apparent stress σ_a, there is a model-dependent discrepancy between the σ_a inferred from theoretical energy partitioning and the σ_a predicted using spherical mean corner frequency. Their ratio c_p varies significantly from 1.0 for the Brune (1970, 1971) model to 6.38 for the Madariaga (1976) model. If one uses spectral models to predict the ground motion, c_p must be considered. (3) We infer that the constancy of the "stress parameter" ($\widetilde{\Delta\sigma}$) found in engineering seismology (e.g., Boore, 1983; Atkinson and Beresnev, 1998) is similar to having constant apparent stress, σ_a (e.g., Ide and Beroza, 2001). The observation that $\widetilde{\Delta\sigma}$ is generally larger than the average static stress drop $\Delta\sigma_s$ for global M > 5.5 shallow crustal earthquakes in active tectonic regions implies that these earthquakes radiate, on average, more seismic energy than predicted from the conventional dynamic crack models.

KEY POINTS

- $\Delta\sigma_s$ estimated using the conventional M_0 & f_c methods strongly depend on the particular theoretical spectral model.
- Model-dependent variability of spectral estimates of $\Delta\sigma_s$ can be largely reconciled using radiated energy E_R.
- Robust stress drop estimates are important for seismological studies and engineering applications.

INTRODUCTION

Static stress drop, which represents the stress difference across the fault surface before and after an earthquake, is an important physical source parameter and has been studied extensively in seismology. The static stress drop of an earthquake often varies locally over its fault surface. Because of the limited resolution of geophysical data, only the spatial average over the coseismic rupture surface can be accessed in most circumstances. Many variants of the average stress drop definition have been introduced in the literature (e.g., Noda *et al.*, 2013). Using them interchangeably is often a source of confusion. In this note, we use $\Delta\tau(\xi)$ to represent the static stress drop at one point ξ on the fault surface and specifically refer to $\Delta\sigma_s$ as the average static stress drop defined as

$$\Delta\sigma_s = C_A M_0 / A^{\frac{3}{2}}, \quad (1)$$

in which A represents the coseismic rupture area, and M_0 is the seismic moment. C_A is a constant related to the shape of the rupture plane (Aki, 1972; Noda *et al.*, 2013); it varies less than 20% when the aspect ratio of the rupture plane is smaller than four (Noda *et al.*, 2013). This definition of $\Delta\sigma_s$ is also used in Brune's (1970) spectral method. Using equation (1), Kanamori and Anderson (1975) reported $\Delta\sigma_s$ of 3 MPa for the mean average static stress drop for interplate and 10 MPa for intraplate earthquakes. Their result has been affirmed by many later studies (e.g., Kanamori, 1978; Wells and Coppersmith, 1994; Hanks and Bakun, 2008; Irikura and Miyake, 2010; Leonard, 2010; Murotani *et al.*, 2015). However, the peak static stress drop on the fault surface, that is, the maximum of $\Delta\tau(\xi)$, can be significantly larger (e.g., Brune, 1970; Bouchon, 1997; Ripperger and Mai, 2004; Irikura and Miyake, 2010; Brown *et al.*, 2015).

1. Department of Earth Science, University of California, Santa Barbara, California, U.S.A., https://orcid.org/0000-0002-0350-5704 (CJ); https://orcid.org/0000-0003-4902-5412 (RJA); 2. Earth Research Institute, University of California, Santa Barbara, California, U.S.A.; 3. Southern California Earthquake Center, University of Southern California, Los Angeles, California, U.S.A., https://orcid.org/0000-0003-1121-7726 (YW)

*Corresponding author: ji@geol.ucsb.edu

Cite this article as Ji, C., R. J. Archuleta, and Y. Wang (2022). Variability of Spectral Estimates of Stress Drop Reconciled by Radiated Energy, *Bull. Seismol. Soc. Am.* **XX**, 1–15, doi: 10.1785/0120210321

Because of the challenge in determining rupture area A, most estimates of $\Delta\sigma_s$, particularly for small and even moderate-magnitude earthquakes, have been made using the corner frequency f_c of the observed source spectra (e.g., Ide *et al.*, 2003; Shearer *et al.*, 2006; Mayeda *et al.*, 2007; Oth *et al.*, 2010; Shearer *et al.*, 2019; Abercrombie *et al.*, 2021; Shearer and Abercrombie, 2021), following the seminal work of Brune (1970). We hereafter refer to this stress drop estimate as $\Delta\sigma_{f_c}$. However, depending on which theoretical model is used (e.g., Brune, 1970; Sato and Hirasawa, 1973; Madariaga, 1976; Kaneko and Shearer, 2014; Wang and Day, 2017), the inferred stress estimate for the same source spectrum can differ by a factor of 5.56. A numerical agreement of stress drop $\Delta\sigma_{f_c}$ may imply a large discrepancy. For instance, Allmann and Shearer (2009) conducted a global survey for stress drop of $M_w > 5.5$ earthquakes using the observed P-wave spectra from seismograms at teleseismic distances. They reported a median stress drop of 4.6 MPa using Madariaga's (1976) relation (assuming a shear-wavespeed of 3500 m/s at the source region). Baltay and Hanks (2014) showed that the mean peak ground accelerations (PGAs) and mean peak ground velocities (PGVs) for stations close to the faults for shallow crustal earthquakes (SCEs) in tectonically active regions can be matched with a stress drop of 4.64 MPa in a point source stochastic procedure and Brune's spectral model (Brune, 1970). Their stress drop is 25 MPa if one uses Madariaga's relation instead of Brune's. This difference begs the question: How does one reconcile such a big discrepancy? Are the near- and far-field radiation so different, or is something missed in the earlier interpretation?

The stress drop used during stochastic ground motion simulations has often been referred to as "stress parameter" (hereafter referred to $\widetilde{\Delta\sigma}$; Boore, 1983) in the bulk of engineering seismology literature. The discrepancy between values of $\widetilde{\Delta\sigma}$ and $\Delta\sigma_s$ has been reported (e.g., Hanks and McGuire, 1981; Boore, 1983). It led Atkinson and Beresnev (1998) to a well-known letter entitled "do not call it stress drop", in which they argued that $\widetilde{\Delta\sigma}$ may bear no relationship to real stresses on the fault surface. What does this important parameter in engineering seismology mean? Cotton *et al.* (2013) pointed out that the between-event variation of $\widetilde{\Delta\sigma}$ inferred from various ground motion prediction equations is much smaller than the between-event variation of stress drop estimated using source spectra (e.g., Allmann and Shearer, 2009). Understanding the physical meaning of $\widetilde{\Delta\sigma}$ could allow one to take advantage of its well-behaved magnitude independence that was recognized four decades ago (Hanks and McGuire, 1981).

In this study, we attempt to explore the theoretical and empirical relations among $\Delta\sigma_s$, $\Delta\sigma_{f_c}$, and $\widetilde{\Delta\sigma}$. Considering the notable uncertainties related to various stress measurements (e.g., Leonard, 2010; Cotton *et al.*, 2013), in this preliminary work, we further restrict our attention to the relations between their means for earthquakes with the same magnitude. Because the measurements of $\Delta\sigma_s$ (defined as equation 1) are only available for a few small or moderate earthquakes (e.g., Dreger *et al.*, 2007), the observational results of large ($M_w > 5.5$) earthquakes in literature are used. Our effort can be further divided into the following three parts.

We first reexamine the original articles of several theoretical source spectral models. One major feature stands out. Despite the large difference (up to a factor of 5.56) in stress drop estimates from different spectral models, there is a remarkable consistency in seismic radiation efficiency η_R (Brune, 1970; Madariaga, 1976; Kaneko and Shearer, 2014; Wang and Day, 2017). All models predict that earthquakes radiate about half of their available strain energy to the surrounding medium. This consistency strongly suggests using seismic radiated energy E_R (or apparent stress $\sigma_a = \mu\frac{E_R}{M_0}$, μ is rigidity, Wyss and Brune, 1968) as an anchor when comparing different spectral models. We show that, in theory, how an E_R-based method for estimating stress drop is less model dependent than the conventional methods.

Second, when researchers forward predict ground motion using source spectral models and stress drop (e.g., Hanks and McGuire, 1981; Boore, 1983), a point source approximation has to be applied. We notice an interesting fact that is embedded in nearly all source spectral models except Brune's (1970). The corner frequency f_c that is used to solve for stress drop $\Delta\sigma_{f_c}$ cannot correctly predict the corresponding radiated seismic energy E_R or apparent stress σ_a. To conserve E_R under such a point source approximation, a E_R-based corner frequency $f_c^{E_R}$ for a given spectral model is introduced. Taking this issue into consideration, the "apparent" inconsistency between the aforementioned two well-known studies of global earthquakes (Allmann and Shearer, 2009; Baltay and Hanks, 2014) can be partially explained. In the Discussion section we further outline why the stress parameter $\widetilde{\Delta\sigma}$ can be viewed as another form of apparent stress σ_a under some limitations.

Third, how well an E_R-based stress drop $\Delta\sigma_{E_R}$ approximates static stress drop $\Delta\sigma_s$ depends on apparent seismic radiation efficiency η_R^A ($= 2\sigma_a/\Delta\sigma_s$, e.g., Beeler *et al.*, 2003). We discuss various source parameters that affect the value of η_R^A and conclude that it is difficult to theoretically predict the range of η_R^A. However, extensive measurements of $\Delta\sigma_s$ and σ_a for $M_w > 5.5$ earthquakes are available for which the variability of $\Delta\sigma_s$ and σ_a is much less compared to similar measurements for $M_w < 5.5$ earthquakes (see fig. 1 in Abercrombie, 2021). Especially, the measurements of $\Delta\sigma_s$ and σ_a for many $M_w > 5.5$ earthquakes were constrained using observations other than the corner frequency f_c (Kanamori and Anderson, 1975; Choy and Boatwright, 1995; Leonard, 2010; Kanamori *et al.*, 2020). We show that the mean $\Delta\sigma_{E_R}$ is slightly larger than the mean $\Delta\sigma_s$ for these earthquakes.

This study can help us to better understand the various stress estimates of moderate and large earthquakes in the literature, and shed light on the absolute $\Delta\sigma_s$ of small earthquakes.

A REVIEW OF CONVENTIONAL SOURCE MODELS

In this short note, we will focus on four articles that provide insights into the source spectra: Brune (1970), Madariaga (1976), Kaneko and Shearer (2014), and Wang and Day (2017). The Brune model (Brune, 1970, 1971) and the Madariaga model (Madariaga, 1976) are the most widely used source spectral models in the seismological literature. The results of Kaneko and Shearer (2014) and Wang and Day (2017) represent recent developments in this field. All models adopted a whole space approximation to the earth medium. Because our attention is focused on SCEs in active tectonic regions (Ancheta *et al.*, 2014), we use $\beta = 3500$ m/s and $\rho = 2700$ kg/m^3 as S wavespeed and density at the source region. The default rigidity μ is then 3.3×10^4 MPa.

All of these models considered rupture on a circular fault plane and estimated the average stress drop $\Delta\sigma_s$ using Eshelby's relation (Eshelby, 1957):

$$\Delta\sigma_s = \left(\frac{7}{16}\right)(M_0/a^3), \tag{2}$$

in which M_0 is the seismic moment, and a is the radius. This is equivalent to equation (1) with $C_A = 2.44$. When spatially heterogeneous slip and stress drop on a fault are known, it is useful to estimate the energy-based (or slip weighted) average static stress drop $\Delta\sigma_s^E$ (Noda *et al.*, 2013):

$$\Delta\sigma_s^E = \frac{\int_A \Delta\tau(\xi)\cdot\mathbf{D}(\xi)dA}{\int_A \mathbf{D}(\xi)dA}, \tag{3}$$

where $\Delta\tau(\xi)$ and $\mathbf{D}(\xi)$ represent the static stress drop and slip at a point ξ on the fault surface in vectors. $\Delta\sigma_s^E$ can be estimated with available finite fault slip models (e.g., Shao *et al.*, 2012; Ye *et al.*, 2016). However, it is sensitive to small-scale slip or stress variations, and only its lowest bound can be constrained with geophysical observations (Adams *et al.*, 2019). Kikuchi and Fukao (1988) and Noda *et al.* (2013) proved $\Delta\sigma_s^E \geq \Delta\sigma_s$. These two measures of average stress drop are equal when $\Delta\tau(\xi)$ is a constant on the fault.

Brune (1970) introduced an idealized representation for the earthquake source spectrum as

$$\Omega_0(f) = M_0/\left(1 + \left(\frac{f}{f_c}\right)^\gamma\right), \tag{4}$$

in which f_c is corner frequency, and $\gamma = 2$ is the high-frequency falloff rate. The asymptotic amplitude of this spectrum is proportional to the seismic moment M_0 at low frequency and decays as f^{-2} at high frequency. Brune (1970) also introduced an ad hoc time-domain source time function, $\Omega_0(t) = M_0\omega_c^2 te^{-\omega_c t}$, $\omega_c = 2\pi f_c$ and $t > 0$, which has the same spectral shape as equation (4). The duration of $\Omega_0(t)$ is infinite, but 95% of its seismic moment (M_0) occurs in the interval $[0, 0.755/f_c]$. Brune (1970) modeled an earthquake as a circular fault with simultaneous, constant stress relaxation over the entire fault, that is, infinite rupture velocity. Adopting a point source approximation and an argument analogous to the conservation of total "seismic radiated energy," Brune (1970) derived a relation between f_c and the source radius a, and subsequently tectonic effective stress (dynamic stress drop) $\Delta\sigma_d$:

$$f_c = k\frac{\beta}{a}, \tag{5a}$$

$$\Delta\sigma_d = \frac{7M_0}{16}[f_c/(k\beta)]^3, \tag{5b}$$

in which β is the S wave velocity in the source region and $k \sim 0.372$. Brune (1970) only considered S-wave radiation and assumed implicitly $\Delta\sigma_d = \Delta\sigma_s$ so that he could use equation (2) to link $\Delta\sigma_d$ with M_0. In the following discussion, we refer to the methods that use equations (5a) and (5b) or its variants to estimate $\Delta\sigma_s$ from seismic moment and corner frequency as M_0 & f_c methods and the corresponding solutions of stress drop as $\Delta\sigma_{f_c}$. Specifically, we refer to $\Delta\sigma_{f_c}$ estimated using Brune's k value of 0.372 as Brune stress drop $\Delta\sigma_{f_c}^{\mathrm{B}}$.

The rupture front of an earthquake propagates with a finite rupture velocity V_R. Madariaga (1976) studied a quasi-dynamic (stress relaxation but rupture velocity prescribed) circular crack that radially expands with $V_R = 0.9\beta$. He found that the observed corner frequencies vary with the takeoff angles relative to the fault plane (referred as azimuth in Madariaga, 1976). The corner frequency is "inversely proportional to the width of the far-field displacement pulse, which, in turn, is related to the time lag between the stopping phases" (Madariaga, 1976). Madariaga (1976) attempted to connect the spherical mean of corner frequencies, $\bar{f}_c$ with $\frac{\beta}{a}$ as in equations (5a) and (5b). He obtained a k value of 0.21 for S-wave spectra. We hereafter refer to $\Delta\sigma_{f_c}$ estimated using Madariaga's k value as Madariaga stress drop $\Delta\sigma_{f_c}^{\mathrm{M}}$. As shown in equations (5a) and (5b), $\Delta\sigma_{f_c}$ is proportional to k^{-3}. The difference in k value between Brune (1970) and Madariaga (1976) leads to a factor of 5.56 difference between $\Delta\sigma_{f_c}^{\mathrm{B}}$ and $\Delta\sigma_{f_c}^{\mathrm{M}}$ (Table 1). $\Delta\sigma_{f_c}^{\mathrm{M}}$ is a measure of $\Delta\sigma_s$ rather than $\Delta\sigma_d$. Madariaga (1976) noted that when $V_R = 0.9\beta$, $\Delta\sigma_s = 1.2\sigma_d$, that is, stress overshoot.

Kaneko and Shearer (2014) conducted quasi-dynamic calculations similar to Madariaga (1976) but considered cohesive-zone models, that is, a circularly expanding stress relaxation with a small-scale yielding limit. Kaneko and Shearer (2014) obtained k = 0.26 for S-wave spectra when $V_R = 0.9\beta$. This k is 24% greater than Madariaga's k but still smaller than Brune's. We refer to the $\Delta\sigma_{f_c}$ estimated using this k value as K&S stress drop $\Delta\sigma_{f_c}^{\mathrm{KS}}$. $\Delta\sigma_{f_c}^{\mathrm{KS}}$ is 2.9 times larger than $\Delta\sigma_{f_c}^{\mathrm{B}}$ (Table 1). Again $\Delta\sigma_{f_c}^{\mathrm{KS}}$ is an estimate of $\Delta\sigma_s$. Kaneko and Shearer (2015) reported that when

TABLE 1
Comparisons of Dynamic Circular Crack and Slip Pulse Models

Parameters	Brune Model	Madariaga Model	K&S Model	W&D Models		
				EC	GP	SS
$V_R(\times\beta)$	∞	0.9	0.9	0.84–0.88	0.81–0.85	0.74–0.78
k^s	0.372	0.21	0.26	0.27	0.36	0.31
$(k^s)^{-3}/19.425$	1.0	5.56	2.93	2.62	1.10	1.73
η_R	0.466*	0.533	0.48	0.40	0.65	0.46
$\Delta\sigma_s^E/\Delta\sigma_s$	1	1	1	1	1.31	1.39
η_R^A	0.466	0.533	0.48	0.40	0.85	0.64
$\Delta\sigma_s$ (if $\sigma_a = 1$ MPa)	4.29	3.75	4.17	5.0	2.35 (3.08)†	3.13 (4.35)†
Correction factor (c_p)	1	6.38	3.03	2.25	2.02 (1.54)†	2.38 (1.71)†
$f_c^{E_R}(\times\bar{f}_c)$	1	1.85	1.45	1.31	1.26 (1.16)†	1.33 (1.20)†
k^{E_R}	0.372	0.390	0.377	0.354	0.454	0.412

AP, arresting pulse (Wang and Day, 2017); EC, expanding crack; GP, growing pulse; K&S, Kaneko and Shearer (2014, 2015); SS, steady-state pulse; W&D, Wang and Day (2017).
*Brune model only considered the *S*-wave radiation (Brune, 1970).
†Value inside the parentheses is the estimate by further assuming $\Delta\sigma_s^E = \Delta\sigma_s$.

$V_R = 0.9\beta$, $\Delta\sigma_s = 1.26\Delta\sigma_d$, slightly larger stress overshoot than Madariaga's (1976).

Wang and Day (2017) simulated four simplified spontaneously propagating dynamic rupture models. All the four models are under the same background stress conditions—a statically strong but dynamically weak fault. Depending on the value of the weakening slip velocity, a parameter of the rate and state friction law incorporating a strong velocity weakening mechanism (e.g., flash heating and thermal pressurization), the models are either expanding crack or self-healing pulse-like ruptures (see Wang and Day, 2017 for details). Differing from the numerical studies of Madariaga (1976) and Kaneko and Shearer (2014), the rupture velocity in the Wang and Day (2017) simulations is determined as part of the solution rather than being preassigned. Wang and Day (2017) noted that (1) the rupture velocity has to be slightly different in inplane and antiplane directions (Day, 1982); and (2) static stress drop $\Delta\tau(\xi)$ is notably heterogeneous, especially for the slip-pulse models (see figs. 5, 6, and 7 in Wang and Day, 2017). Their calculation for a spontaneously expanding crack (EC) with $V_R = (0.84 - 0.88)\beta$ (EC, Table 1) resulted in a k value of 0.27, similar to Kaneko and Shearer (2014). A stress overshoot was also observed, $\Delta\sigma_s \sim 1.12\Delta\sigma_d$ (Wang and Day, 2017). Wang and Day (2017) presented three representative self-healing pulse-like modes: growing pulse (GP), steady-state pulse (SS), and arresting pulse (AP). Here we consider only GP and SS models. The AP simulation stops spontaneously before the rupture front reaches the imposed velocity-strengthening barrier, resulting in an elliptical rupture surface (Wang and Day, 2017). The k inferred from these two self-healing pulse-like models is 0.36 for GP and 0.31 for SS, closer to Brune's k. We refer to the $\Delta\sigma_{f_c}$ estimated using these two k values as $\Delta\sigma_{f_c}^{\mathrm{WD}}$, which is 1.10–1.73 times larger than $\Delta\sigma_{f_c}^{\mathrm{B}}$ (Table 1). Because the faulting models of Wang and Day (2017) depend on background stress conditions and the parameters of rate and state friction law (see fig. 17 in Wang and Day, 2017), it is not completely clear whether the results for k are magnitude independent, that is, self-similar, as the crack models.

Regardless of the large discrepancy in the inferred $\Delta\sigma_{f_c}$ among the four crack models for a given pair of corner frequency f_c and seismic moment M_0 (Table 1), all of these models agree in their estimate of seismic radiation efficiency η_R, which is the ratio of seismic radiated energy E_R and the available strain energy ΔW (e.g., Husseini and Randall, 1976; Venkataraman and Kanamori, 2004):

$$\Delta W = \frac{1}{2}\int \Delta\tau(\xi)D(\xi)dA = E_R + \int G(\xi)dA, \tag{6a}$$

$$\eta_R = E_R/\Delta W, \tag{6b}$$

in which $D(\xi)$, $\Delta\tau(\xi)$, and $G(\xi)$ are displacement, static stress drop, and fracture energy density, respectively, at a point ξ on the fault surface. $E_R = E_R^s + E_R^P$ represents the seismic radiated energy carried by S waves and P waves, respectively. Because E_R^P is much smaller than E_R^s (e.g., Kaneko and Shearer, 2014; Wang and Day, 2017), we ignore E_R^P in the following discussions. From equation (2), we have $\Delta W = M_0\Delta\sigma_s^E/2\mu$ (Shao *et al.*, 2012; Noda *et al.*, 2013; Wang and Day, 2017). Equation (6b) can be rewritten as

$$\sigma_a = \frac{1}{2}\left(\frac{\Delta\sigma_s^E}{\Delta\sigma_s}\right)\eta_R\Delta\sigma_s, \tag{7}$$

in which $\sigma_a = \mu\frac{E_R}{M_0}$ (μ is rigidity) is apparent stress (Wyss and Brune, 1968). Adopting a point source approximation and a source spectrum defined in equation (4), σ_a of an earthquake

can also be calculated using f_c and M_0 (e.g., Andrews, 1986; Madariaga, 2011):

$$\sigma_a \cong \frac{\pi^2}{5\beta^3} f_c^3 M_0, \tag{8}$$

in which only E_R^s is taken into account.

In his seminal work, Brune (1970, 1971) reported $\eta_R \sim 0.466$ (only E_R^s was considered; Table 1). Using equation (36) of Madariaga (1976), we obtain $\eta_R \sim 0.533$ for Madariaga's model in which $V_R = 0.9\beta$ (Appendix A). Kaneko and Shearer (2014) reported $\eta_R = 0.48$ for their model with $V_R = 0.9\beta$. The difference between the Madariaga and K&S estimates of η_R can be explained by their difference in stress overshoot, that is, $\Delta\sigma_s/\Delta\sigma_d$ (Appendix A). The EC model of Wang and Day (2017) is a spontaneous rupture with a rupture velocity close to 0.9β (Table 1). Wang and Day (2017) reported $\eta_R = 0.40$ (EC, Table 1), which is correlated with its slower rupture velocity $(0.84 - 0.88)\beta$. Nevertheless, for all the four crack models η_R is 0.470 ± 0.047, essentially a constant when we consider the uncertainty of η_R measurements for individual earthquakes (e.g., Venkataraman and Kanamori, 2004). As $\Delta\sigma_s^E = \Delta\sigma_s$ holds for all the crack models, we can estimate $\Delta\sigma_s$ using the relation $\Delta\sigma_s = (2/\eta_R)\sigma_a$. The median of σ_a measurements from global SCEs is about 1.0 MPa, for example, Ide and Beroza (2001). As shown in Table 1, using $\sigma_a = 1.0$ MPa the inferred $\Delta\sigma_s$ varies between 3.75 and 5.0 MPa among the four crack models. This variation of $\Delta\sigma_s$ is much smaller than the model-dependent variation associated with the conventional M_0 & f_c approaches (Table 1).

The η_R of the GP and the SS models is 0.65 and 0.46, respectively (Table 1). Both values are greater than the EC model 0.40 (Table 1). The average rupture velocity of the GP model is $\sim 0.83\beta$ and that of the SS model is $\sim 0.76\beta$. As we discuss later, η_R of GP and SS models is much larger than the η_R of circular or elliptical crack models with comparable rupture velocity. The ratio $\Delta\sigma_s^E/\Delta\sigma_s$ is 1.31 for the GP model and 1.39 for the SS model (Table 1)—a natural consequence of the pulse-like rupture (Wang and Day, 2017). Assuming $\sigma_a = 1.0$ MPa, the predicted $\Delta\sigma_s$ is 2.35 MPa for the GP model and 3.12 MPa for the SS model (Table 1). These $\Delta\sigma_s$ are smaller than the predicted $\Delta\sigma_s$ using the crack models (Table 1). These predicted values of $\Delta\sigma_s$ are consistent with the average $\Delta\sigma_s$ of SCEs (~3 MPa, e.g., Somerville *et al.*, 1999; Hanks, 2002; Leonard, 2010).

A CORRECTION FACTOR c_p FOR POINT SOURCE SPECTRAL MODELS

If the static stress drop $\Delta\sigma_s$ and seismic moment M_0 of an earthquake are known, the apparent stress σ_a can be estimated using a selected source spectral model. There are two possible approaches:

1. One can directly use the theoretical seismic radiation efficiency η_R of the selected model (Table 1). The predicted σ_a is $\Delta\sigma_s\eta_R/2$.
2. One can use $\Delta\sigma_s$, M_0, and k of the spectral model to predict the spherical mean corner frequency $\bar{f}_c$ using equation (5b):

$$\bar{f}_c = [(16\Delta\sigma_s)/(7M_0)]^{1/3} k\beta. \tag{9}$$

Using equation (8) with M_0 and $\bar{f}_c$ one can determine σ_a. This approach has been used in the engineering seismology community to estimate the source spectrum for strong ground motion simulation (e.g., Boore, 1983), though the k of Brune's model is generally used.

However, the apparent stress σ_a determined by these two approaches is different for some spectral models. Here, we introduce a correction factor c_p, which is the ratio of the σ_a obtained from these two approaches:

$$c_p = (\Delta\sigma_s\eta_R/2)/((\pi^2/5\beta^3)\bar{f}_c^3 M_0) = (35\eta_R)/(32\pi^2 k^3), \tag{10}$$

in which c_p is a function of model-dependent parameters η_R and k. Among the crack models in Table 1, c_p varies from 1.0 for Brune's model to 6.38 for Madariaga's model. The c_p of the two slip pulse models of Wang and Day (2017) are roughly the same: 2.02 for the EP model and 2.38 for the SS model. Because $\sigma_a = \mu\frac{E_R}{M_0}$, a source spectral model with $c_p > 1$ means that when one uses this model to predict the seismic radiated energy E_R through the second approach, the predicted E_R is a factor of c_p smaller than the theoretical expectation.

The large c_p that is associated with the conventional spectral models such as Madariaga's can be explained intuitively. The dynamic crack has a finite size; approximating it as a point source can produce artifacts. Madariaga (1976) and Kaneko and Shearer (2014) showed that both f_c and the high-frequency falloff rate γ vary with the takeoff angle. Differences in f_c and γ lead to the differences in seismic radiated energy density. Let us temporarily assume γ is 2. The energy density is then proportional to f_c^3 for every takeoff angle (equation 8). Let $\bar{f}_c$ be the spherical mean of f_c (Madariaga, 1976; Kaneko and Shearer, 2014; Wang and Day, 2017). Using $\bar{f}_c$ to estimate the cumulative radiated seismic energy is equivalent to using the cube of the spherical mean of f_c, that is, $(\bar{f}_c)^3$ to approximate the spherical mean of f_c^3, that is, $\overline{f_c^3}$. Because $(\bar{f}_c)^3 \le \overline{f_c^3}$ holds for any set of positive f_c, the predicted total seismic radiated energy must be underestimated. The cumulative effect, which is a combined result of variations in f_c, radiation pattern, and falloff decay rate, is a factor as large as 6.38—a factor too large to be ignored. When one uses $\Delta\sigma_s$ and M_0 to predict the seismic radiated energy or high-frequency seismic radiation for engineering applications (Hanks and McGuire, 1981; Boore, 1983), the result must be properly scaled to conserve the total seismic radiated energy.

It should be noted that Brune (1970) considered the balance between the total "energy" radiating from the source and the

total "energy" passing through the surface of a sphere in the far field. Thus, Brune (1970) used $(\overline{f_c^3})^{1/3}$ rather than $\bar{f}_c$ in equations (5a) and (5b), that is, $(\overline{f_c^3})^{1/3} = k\beta/a$. c_p is then 1.0 for the Brune model. We can adopt Brune's energy balance approach to introduce a seismic radiated energy E_R-based k^{E_R} for any spectral model. k^{E_R} can be represented as $c_p^{1/3}k$, in which k is the original constant of a particular spectral model. As shown in Table 1, k^{E_R} ranges from 0.354 to 0.390 among the four crack models, close to Brune's k of 0.372. k^{E_R} is 0.45 and 0.41 for GP and SS models, respectively. The E_R-based k^{E_R} leads to a E_R-based corner frequency (equation 9) that needs to be used for forward prediction when using a particular spectral model. We refer to it as $\bar{f}_c^{E_R}$ with $\bar{f}_c^{E_R} = c_p^{1/3}\bar{f}_c$, in which $\bar{f}_c$ is the spherical mean corner frequency. One can estimate stress drop $\Delta\sigma_{f_c}$ using $\bar{f}_c^{E_R}$ and k^{E_R} as the inputs of equations (5a) and (5b), respectively. The result is same as that using $\bar{f}_c$ and k. But the single corner Brune spectrum (equation 4) with $\bar{f}_c^{E_R}$ as its corner frequency can correctly forward predict the total seismic radiation energy E_R.

Allmann and Shearer (2009) used the M_0 & f_c method to determine the Madariaga stress drop $\Delta\sigma_{f_c}^{\mathrm{M}}$, yielding a median $\Delta\sigma_{f_c}^{\mathrm{M}}$ of 4.6 MPa for global $M_{\mathrm{w}} > 5.5$ shallow earthquakes. Here the $\Delta\sigma_{f_c}^{\mathrm{M}}$ value has been corrected for S-wave velocity at the source region equal to 3500 m/s. Baltay and Hanks (2014) found that a Brune stress drop of 4.64 MPa is optimal to explain the mean PGAs and mean PGVs for stations close to the faults for SCEs. We can also use Madariaga stress drop $\Delta\sigma_{f_c}^{\mathrm{M}}$ of 4.6 MPa (Allmann and Shearer, 2009) to predict the corner frequency for the strong ground motion prediction. As mentioned earlier, we need to use energy-based corner frequency $\bar{f}_c^{E_R}$ rather than $\bar{f}_c$, the spherical mean corner frequency predicted using equation (9) and Madariaga's k. From Table 1, $\bar{f}_c^{E_R} = 1.85\bar{f}_c$. For any given magnitude, this $\bar{f}_c^{E_R}$ is only 4.6% larger than the corner frequency predicted using a $\Delta\sigma_{f_c}^{\mathrm{B}}$ of 4.64 MPa (Baltay and Hanks, 2014), equation (9), and Brune's k. The similarity in the corner frequency leads to the similarity in predicted strong ground motion parameters. The source spectrum using Madariaga stress drop $\Delta\sigma_{f_c}^{\mathrm{M}}$ of 4.6 MPa (Allmann and Shearer, 2009) will also produce a satisfactory explanation for the observed mean PGAs and mean PGVs. Hence, from a perspective of conserving total radiated seismic energy, the agreement in stress value between these two studies is expected. Both suggest that the average static stress drop $\Delta\sigma_s$ is about 4.6 MPa. However, all of our discussions are based on Brune's omega-square source spectral model (equation 4). The spectral model adopted by Allmann and Shearer (2009) has a high frequency fall-off rate γ of 1.6. Numerical analysis has shown that the $\bar{f}_c$ value of an earthquake determined by the conventional spectra fitting method is sensitive to the preassigned γ value (see table 1 of Kaneko and Shearer, 2015). Furthermore, the mean stress drop of 4.6 MPa is about 50% larger than the mean $\Delta\sigma_s$ of global large earthquakes based on seismic moment and fault rupture area (e.g., Kanamori and Anderson, 1975). This discrepancy is discussed later.

We can directly estimate $\bar{f}_c^{E_R}$ with observations, using the robust method proposed by Snoke (1987). For a given S-wave displacement record $u(t)$, Snoke (1987) suggested calculating J, which is the integral of the square of the observed ground velocity $(\dot{u}(t)^2)$. Based on Parseval's theorem, J is the second moment of the power spectrum, which is proportional to the seismic radiated energy density associated with its ray path. Through the conservation of seismic radiated energy, Snoke (1987) derived an analytic relation between J and the corner frequency f_c of an equivalent Brune displacement spectrum (equation 4). He obtained $f_c = [J/(2\pi^3\Omega_0^2)]^{\frac{1}{3}}$, Ω_0 is the long frequency asymptote of the corresponding displacement spectrum. Apparently, under a point source approximation f_c of Snoke method is exactly the E_R-based corner frequency $\bar{f}_c^{E_R}$defined earlier. Kaneko and Shearer (2015) evaluated Snoke's method using synthetic data of their dynamic crack model with $V_R = 0.9\beta$. They found that the f_c defined by Snoke's method is less dependent on the takeoff angle than the conventional spectral fitting method. The corresponding k value using Snoke's method is 0.36 for S-wave spectra (Kaneko and Shearer, 2015), which is much larger than K&S's k (0.26, Table 1) but nearly identical with the theoretical E_R-based k^{E_R} for the K&S model (0.376, Table 1) and with Brune's k (0.372). Using k = 0.36 and $\eta_R = 0.48$ in equation (10), we obtain $c_p = 1.14$. It suggests that the f_c estimated using Snoke's method is only 4.3% smaller than the theoretical $\bar{f}_c^{E_R}$ for the K&S model (Table 1). Using this f_c to approximate $\bar{f}_c^{E_R}$, the estimate of E_R is about ($12\% = 1 - \frac{1}{c_p}$) smaller than the corresponding theoretical value. This negligible discrepancy affirms the argument that the f_c defined by Snoke's method is less dependent on the takeoff angle (Kaneko and Shearer, 2015). Only under this condition, $(\bar{f}_c)^3 \sim \overline{f_c^3}$ holds. For a comparison, observational studies often assume an omega-square source spectrum when conducting spectra fitting (e.g., Ide *et al.*, 2003; Mayeda *et al.*, 2007; Baltay *et al.*, 2011). Kaneko and Shearer (2015) also test this approach using the same synthetic data. They obtained k = 0.34, again closer to k^{E_R} than the k of the K&S model. The corresponding f_c is about 10% smaller than the theoretical $\bar{f}_c^{E_R}$ for the K&S model (Table 1). Using this alternative approach, the E_R estimate is then 26% smaller. This approach is then slightly worse than Snoke's method.

Using the $\bar{f}_c^{E_R}$ estimated with Snoke's method, k^{E_R}, and equation (5b), one can estimate static stress drop, which we name E_R-based static stress drop $\Delta\sigma_{E_R}$. The model dependency of k^{E_R} leads to the model dependency of $\Delta\sigma_{E_R}$. We use $\Delta\sigma_{E_R}^{\mathrm{B}}$, $\Delta\sigma_{E_R}^{\mathrm{M}}$, and $\Delta\sigma_{E_R}^{\mathrm{KS}}$ for Brune's, Madariaga's, and K&S's model, respectively. $\Delta\sigma_{E_R}^{\mathrm{B}}$ was originally proposed by Snoke (1987) as a relatively robust way to estimate Brune's stress drop. Because k^{E_R} of these three models (Table 1) are remarkably close, the relative differences among $\Delta\sigma_{E_R}^{\mathrm{B}}$, $\Delta\sigma_{E_R}^{\mathrm{M}}$, and $\Delta\sigma_{E_R}^{\mathrm{KS}}$ are less than 15%. We select $\Delta\sigma_{E_R}^{\mathrm{B}}$ as their representative value.

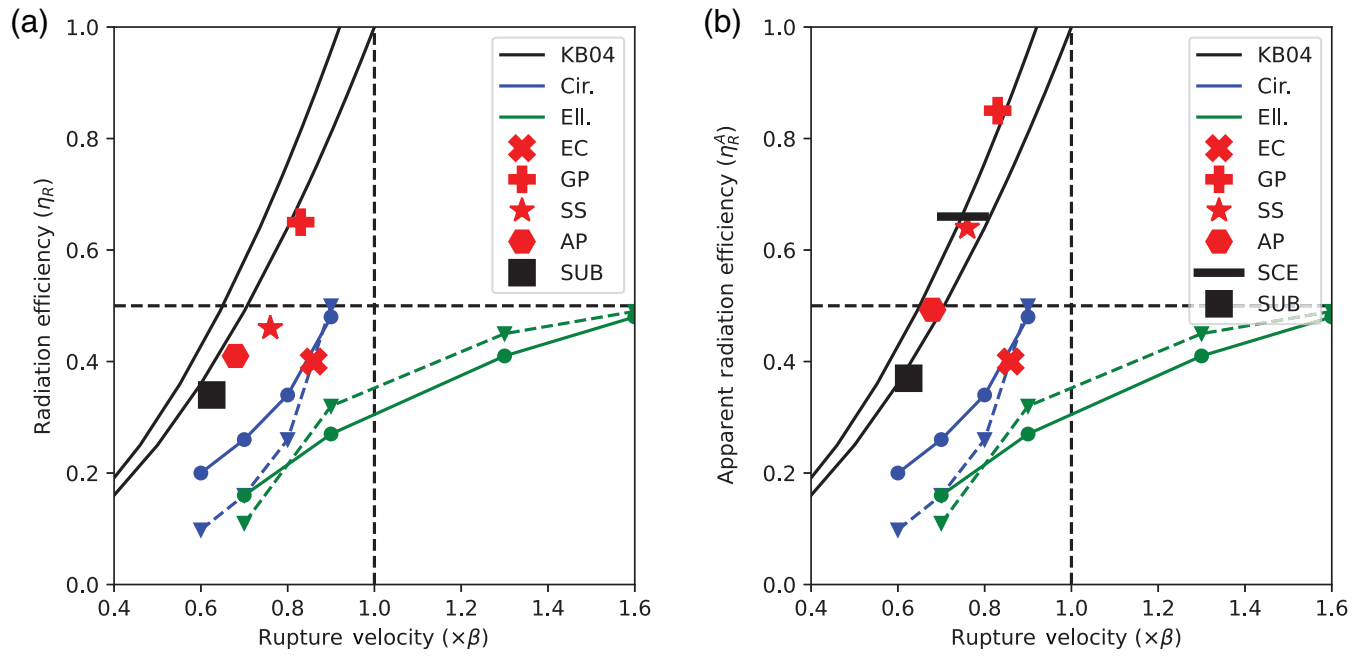

Figure 1. (a) Dependency of seismic radiation efficiency η_R and (b) apparent seismic radiation efficiency η_R^A on rupture velocity. The vertical dashed line divides the plot into subshear and supershear rupture velocity regions. The horizontal dashed line, $\eta_R^A = 0.5$, highlights the uppermost bound of circular or elliptical crack models with near homogeneous stress drop distribution. The predictions using model KB04 (Kanamori and Brodsky, 2004) with limiting rupture velocity C_L of 0.92β and β are presented as solid black lines. The results of Kaneko and Shearer (2015) are shown in blue for rupture scenarios on circular fault planes and in green for rupture scenarios on elliptical fault planes. The filled circles and solid color lines are used for radial or bilateral rupture propagation; filled triangles and dashed lines are for unilateral rupture. The red symbols represent the three rupture modes of Wang and Day (2017) with EC: expanding crack, GP: growing pulse, and SS: steady-state pulse. For comparison, in (a) the black square denotes the geometric mean η_R of large shallow subduction earthquakes reported in Ye *et al.* (2016) (rupture velocity is 2.5 km/s; average shear-wave velocity at source centroid depth is ~4 km/s, Lingling Ye, personal comm., 2020). In (b) the black bar indicates the η_R^A for a representative shallow crustal earthquake with rupture velocity of $(0.7 - 0.8)\beta$, $\widetilde{\Delta\sigma}$ of 4.64 MPa, and $\Delta\sigma_s$ of 3.0 MPa. The black square shows a representative subduction earthquakes (SUB) event with σ_a of 0.56 MPa (Ye *et al.*, 2016) and $\Delta\sigma_s$ of 3.0 MPa. See Variations of Seismic Radiation Efficiency η_R and Heterogeneous Static Stress Drop Distribution and Apparent Radiation Efficiency (η_R^A) for details.

DISCUSSION

Snoke (1987) pointed out that ignoring the contribution of *P*-wave radiation and directivity effect, $\Delta\sigma_{E_R}^B$ is a constant multiple of apparent stress σ_a, that is, $\Delta\sigma_{E_R}^B/\sigma_a = 2/\eta_R \sim 4.3$ (Table 1). The similarity in seismic radiation efficiency η_R among the conventional spectral models (Table 1) leads to relatively model-independent E_R-based stress drop $\Delta\sigma_{E_R}$. For natural earthquakes the agreement between $\Delta\sigma_{E_R}^B$ and $\Delta\sigma_s$, however, will depend on how well the η_R of an earthquake agrees with Brune's model (0.466, Table 1). As shown next, the value of η_R is sensitive to many source parameters.

Variations of seismic radiation efficiency η_R

Previous theoretical studies have shown that η_R (the ratio between seismic radiated energy E_R and the available strain energy ΔW) is positively correlated with rupture velocity V_R (e.g., Husseini and Randall, 1976; Venkataraman and Kanamori, 2004; Kanamori and Rivera, 2006). Kaneko and Shearer (2015) examined a variety of crack rupture scenarios for circular and elliptical faults with constant V_R ranging from 0.6β to 1.6β (Fig. 1). They reported that for a radially propagating rupture on a circular fault, η_R decreases from 0.48 to 0.20 when V_R decreases from 0.9β to 0.6β (blue line, Fig. 1). η_R is also sensitive to fault geometry and symmetric/asymmetric rupture style. For the scenarios with $V_R = 0.7\beta$, a reasonable value for SCEs (Kanamori, 1994), η_R decreases from 0.26 for a symmetric rupture expansion on a circular fault to 0.16 for an asymmetric rupture expansion on a circular fault or a symmetric rupture expansion on an elliptical fault. η_R decreases even more to 0.11 for an asymmetric rupture expansion ($V_R = 0.7\beta$) on an elliptical fault (Kaneko and Shearer, 2015). The mean η_R of these four scenarios is 0.17—about one-third of η_R for a circular expanding crack ($V_R = 0.9\beta$) (Fig. 1a). The maximum η_R found by Kaneko and Shearer (2015) is 0.5. Based on the results of Kaneko and Shearer (2015) we would conclude that the $\eta_R \sim 0.5$, representative of the three conventional source spectral models—Brune, Madariaga, and K&S (Table 1)—is essentially an upper bound on η_R for a propagating crack-type rupture on elliptical faults with constant V_R and uniform static stress drop ($\Delta\tau(\xi) =$ constant). This is an important property when we discuss η_R of natural earthquakes.

However, the theoretical relation between η_R and V_R is model dependent. Kanamori and Brodsky (2004) considered a propagating crack that is driven by the stress concentration near the crack tip. They suggested a simple $\eta_R - V_R$ relation based on energy balance consideration: $\eta_R = (V_R/C_L)^2$, C_L is the limiting rupture velocity, 0.92β (Rayleigh wavespeed) orβ, assuming subshear rupture propagation (black lines, Fig. 1). This relation is generally consistent with the similar relations for the rupture propagation of mode I, II, and III cracks (Kanamori and Rivera, 2006). However, for the given rupture velocity V_R it predicts a much larger η_R than found for any of the crack models (Fig. 1a). This difference probably reflects the difference in the fracture energy density distribution. The fracture energy density (the energy per unit fault surface needed to advance the rupture front, Madariaga, 1976) is constant on the fault plane in the models of Kanamori and Brodsky (2004) but increases with the rupture propagation distance in the dynamic crack models (Madariaga, 2011; Kaneko and Shearer, 2014).

The 3D spontaneous dynamic simulations using the rate and state friction law result in both crack and slip-pulse rupture scenarios, dependent on the value of slip weakening velocity (Wang and Day, 2017). The η_R of their EC model is 0.4—considerably smaller than the η_R of three conventional spectral models (0.466–0.533, Table 1). However, the V_R of this model changes from 0.84β to 0.88β with a mean of 0.86β. By interpolating the model predictions of Kaneko and Shearer (2015), we have estimated η_R of a quasi-dynamic crack model with $V_R = 0.86\beta$ and obtained an η_R estimate of 0.42, agreeing with the EC model. On the other hand, the η_R of the slip-pulse models generally are close to the predictions of Kanamori and Brodsky (2004) but slightly smaller (Fig. 1a). In Wang and Day (2017) the fracture energy density for the rate and state friction law is not clearly defined during slip-pulse rupture scenarios, because the sliding friction never reaches a constant during the entire rupture process. Constant fracture energy density or propagational dependent fracture energy density may be viewed as approximations to the two end member rupture modes, that is, slip pulse and crack.

Heterogeneous static stress drop distribution and apparent radiation efficiency (η_R^A).

The η_R used in this study can be rewritten as $2\sigma_a/\Delta\sigma_s^E$ (equation 7) (Noda *et al.*, 2013), related with energy-based average stress drop $\Delta\sigma_s^E$ rather than $\Delta\sigma_s$. We will then refer to $2\sigma_a/\Delta\sigma_s$ as apparent seismic radiation efficiency η_R^A, which is twice the Savage–Wood efficiency (Savage and Wood, 1971; Beeler *et al.*, 2003). Note $\eta_R^A = (\Delta\sigma_s^E/\Delta\sigma_s)\eta_R$. All of the crack models we reviewed have roughly uniform stress drop distributions, that is, $\Delta\tau(\xi) = \Delta\sigma_s$. In these cases, $\Delta\sigma_s^E = \Delta\sigma_s$ and, consequently, $\eta_R^A = \eta_R$. However, decades of finite fault studies have shown that large earthquakes generally have heterogeneous slip and variable static stress drop on the fault (e.g., Heaton, 1990; Mai and Beroza, 2002), that is, $\Delta\tau(\xi) \neq \Delta\sigma_s$. Thus $\Delta\sigma_s^E > \Delta\sigma_s$ (Kikuchi and Fukao, 1988; Noda *et al.*, 2013) and $\eta_R^A > \eta_R$. Practically it is difficult to measure $\Delta\sigma_s^E$ precisely using seismic and geodetic data, because it is sensitive to the small-scale slip heterogeneities (Adams *et al.*, 2017, 2019). Therefore, relative to η_R, η_R^A is a more robust seismological measurement.

Although η_R and η_R^A are often used interchangeably in the literature (e.g., Venkataraman and Kanamori, 2004; Lambert *et al.*, 2021), they can be quite different for earthquakes with heterogeneous rupture. As mentioned earlier, the slip pulse models of Wang and Day (2017) are associated with heterogeneous stress drop distributions; η_R^A of these models is 1.3–1.4 times the corresponding η_R. Using the $\Delta\sigma_s/\sigma_a$ ratios in Table 1, we obtain η_R^A of 0.87 for the GP model and 0.65 for the SS model (Fig. 1b). Somerville *et al.* (1999) analyzed a collection of finite-fault models for SCEs. They found that the cumulative asperity area during an earthquake is about a quarter of the entire rupture area, and about one-half of the total seismic moment is released by the rupture of asperities that have an average slip twice the average slip of the entire fault. This result was confirmed in later studies (Irikura and Miyake, 2010; Asano and Iwata, 2011). The mean static stress drop of the asperities is 10.5 MPa—4.6 times larger than the $\Delta\sigma_s$ of the entire fault (Irikura and Miyake, 2010).

One can estimate $\Delta\sigma_s^E/\Delta\sigma_s$ for a representative earthquake that roughly obeys the scaling relationships of Somerville *et al.* (1999). For convenience of discussion, let us simply assume that this earthquake has a circular fault plane containing one circular asperity. The area, average fault slip, and $\Delta\sigma_s$ of the entire fault are ***A***, ***D***, and 2.3 MPa, respectively. Those of the asperity are 0.25 ***A***, 2.0 ***D***, and 9.2 MPa. The seismic moment of the asperity is half of the entire rupture. It is easy to show that the $\Delta\sigma_s^E$ of this event is as large as 4.6 MPa, even when one assumes zero static stress drop within the region outside the asperity but inside the rupture plane (asperity model, Boatwright, 1988; Irikura and Miyake, 2010). Thus $\Delta\sigma_s^E/\Delta\sigma_s = 2$. If the seismic radiation of the asperity is estimated with Brune's model, as is commonly used in strong ground motion simulation (Graves and Pitarka, 2010; Irikura and Miyake, 2010), the radiated seismic energy from the asperity can be represented as $\Delta\sigma_s^A M_0^A/(4.3\mu)$, in which $\Delta\sigma_s^A$ and M_0^A are static stress drop and seismic moment of the asperity, respectively. It is easily shown that η_R, η_R^A, and apparent stress σ_a of the entire fault are approximately 0.466, 0.932, and 1.1 MPa, respectively. Here, we ignore the contribution from the region outside the asperity but inside the rupture plane (Irikura and Miyake, 2010). We emphasize that η_R^A is twice η_R. Coincidentally, this σ_a is consistent with the mean of global SCEs (e.g., Ide and Beroza, 2001; Baltay *et al.*, 2011; Convers and Newman, 2011; Kanamori *et al.*, 2020). It is important to note that rupture heterogeneities also affect the comer frequency f_c using the conventional spectral fitting methods; f_c was found to be more sensitive to the dominant subevent size than to the overall event size (Boatwright, 1984a).

Two possible mechanisms that could explain the observed heterogeneous static stress drop distributions of global large earthquakes are: (1) the distributions result from preexisting heterogeneities on the fault surface, such as asperities (Lay *et al.*, 1982) and barriers (Aki, 1984); (2) the distributions result from ruptures satisfying a rate and state friction law (Wang and Day (2017). Preexisting on-fault heterogeneities and velocity weakening friction law are also the conventional explanations for the observations that the average rise time of an earthquake is often much smaller than its total rupture duration, that is, slip-pulse (Heaton, 1990; Beroza and Mikumo, 1996). These two mechanisms are indistinguishable when looking at η_R^A.

In summary, although the three conventional source spectral models—Brune, Madariaga, and K&S (Table 1)—predict nearly identical theoretical η_R^A values, many factors can affect the η_R^A. Large earthquakes have predominant unilateral rupture style (McGuire *et al.*, 2002) and slower rupture propagation velocity V_R (0.7–0.8β, Kanamori (1994)). Both lead to decreasing η_R^A compared to the predictions of these conventional spectral models (Fig. 1). In contrast, either preexisting heterogeneities (e.g., Aki, 1984) or slip-pulse behavior (e.g., Heaton, 1990; Wang and Day, 2017) would increase η_R^A compared to the predictions (Fig. 1b). These theoretical considerations can be used to explain the observations but cannot quantitatively predict the range of η_R^A. Estimates of η_R^A for large SCEs are limited and have considerable uncertainties (Venkataraman and Kanamori, 2004; Lambert *et al.*, 2021). Most estimates vary between 0.3 and 1.0 with a few larger than 1.0 (Venkataraman and Kanamori, 2004). If one uses 0.466 of Brune's model to approximate the η_R^A of large SCEs, without additional corrections, one has to accept a factor of 2 uncertainty around the mean, that is, $0.233 < \eta_R^A < 0.932$. This empirical uncertainty in η_R^A leads to uncertainty in $\Delta\sigma_s$ from the $\Delta\sigma_{E_R}^B$ approach (Snoke, 1987). However, this uncertainty is linear with respect to η_R^A, unlike the uncertainty associated with $\Delta\sigma_{f_c}$ that cubes measurement error in corner frequency f_c.

Our general knowledge about SCEs suggests that the mean η_R^A of SCEs may be larger than that predicted by Brune's model. Consider a scenario SCE with $\Delta\sigma_s$ of 3.0 MPa (e.g., Hanks and Bakun, 2008; Leonard, 2010), apparent stress σ_a of 1.0 MPa (e.g., Ide and Beroza, 2001; Baltay *et al.*, 2011; Convers and Newman, 2011; Kanamori *et al.*, 2020), rupture velocity V_R of $0.7\beta - 0.8\beta$ (Kanamori, 1994). The corresponding η_R^A is 0.66, about 40% larger than η_R^A of Brune's model but in agreement with the SS slip-pulse model of Wang and Day (2017; Fig. 1b). On the other hand, the average η_R^A of large shallow interplate subduction earthquakes (SUBs) might be smaller. Ye *et al.* (2016) reported estimates of $\Delta\sigma_s^E$ and σ_a for 114 $M_w > 7$ shallow subduction interplate earthquakes. The geometric means of $\Delta\sigma_s^E$, σ_a, and η_R were 3.44 MPa, 0.56 MPa, and 0.34, respectively (Fig. 1a). If the mean $\Delta\sigma_s$ of SUBs is still 3.0 MPa (Kanamori and Anderson, 1975; Leonard, 2010), η_R^A is 0.37, about 25% less than that of Brune's model.

The physical meaning of "stress parameter"

Boore (1983) introduced the terminology "stress parameter" ($\widetilde{\Delta\sigma}$), following the seminal work of Hanks and McGuire (1981). For a given earthquake, he used $\widetilde{\Delta\sigma}$, seismic moment M_0, and the k value of Brune's model to predict the corner frequency of its source spectrum (equation 9). This source spectrum was subsequently used to predict PGA, PGV, local magnitude, and response spectra successfully. $\widetilde{\Delta\sigma}$ has even since been widely used as a key source parameter during the stochastic strong ground motion simulations (e.g., Atkinson and Boore, 1995; Atkinson and Silva, 1997; Boore, 2003; Graves and Pitarka, 2010; Boore *et al.*, 2014). However, the physical meaning of stress parameter $\widetilde{\Delta\sigma}$ has not been clearly defined. $\widetilde{\Delta\sigma}$ of earthquakes is often different from the corresponding $\Delta\sigma_s$ and $\Delta\sigma_{f_c}^B$ (M_0 & f_c stress drop with Brune's k or Brune stress drop, e.g., Hanks and McGuire, 1981; Boatwright, 1984b; Atkinson and Beresnev, 1998). We surmise that might be the reason why Boore (1983) did not simply call it Brune stress drop.

We emphasize that during such forward stochastic strong ground motion simulations with Brune ω^{-2} source spectra and Brune's k, the analytical relation $\widetilde{\Delta\sigma}/\sigma_a = 2/\eta_R \sim 4.3$ (Andrews, 1986; Singh and Ordaz, 1994) firmly holds. In principle, $\widetilde{\Delta\sigma}$ is simply another form of apparent stress σ_a and shall be equal to $\Delta\sigma_{E_R}^B$. The mean σ_a of $M_w > 5.5$ SCEs was found to be about ~1.0 MPa, independent of magnitude (Ide and Beroza, 2001; Ide *et al.*, 2003; Prieto *et al.*, 2004; Baltay *et al.*, 2011; Convers and Newman, 2011; Kanamori *et al.*, 2020). For a given magnitude, σ_a is log normal distributed with significant log normal standard deviation (0.41 in log10 units, Baltay *et al.*, 2011). Baltay and Hanks (2014) showed that the mean PGA and mean PGV at stations close to the faults for $3 < \mathbf{M} < 8$ shallow earthquakes in tectonically active regions (Ancheta *et al.*, 2014) can be matched with a point source stochastic procedure and Brune's spectral model with $\widetilde{\Delta\sigma}$ of 4.64 MPa. It is equivalent to say that these data can be modeled using Brune ω^{-2} source spectra with an apparent stress σ_a of 1.1 MPa, consistent with the mean σ_a previously reported for global shallow earthquakes. In fact, the mean σ_a may be more robust than $\widetilde{\Delta\sigma}$ because $\widetilde{\Delta\sigma}$ is model dependent. Ji and Archuleta (2020) found that the data studied by Baltay and Hanks (2014) can be well explained using a double-corner frequency (DCF) source spectrum. Although the stress parameter of these DCF models cannot be properly defined, the predicted apparent stress σ_a is 0.73 MPa using self-similar model JA19. If one uses the non-self-similar JA19_2S model, the synthetic σ_a varies slightly from 1.6 to 0.73 MPa when moment magnitude changes from 5.3 to 7.3, with a geometric mean of 1.1 MPa. Ji and Archuleta (2021) also noted that the predicted σ_a of additive DCF spectral model AS00 (for California earthquakes, Atkinson and Silva, 2000) has similar magnitude dependency as JA19_2S (Ji and Archuleta, 2021). On the other hand, the σ_a of additive DCF spectral model AB95 (for eastern North California earthquakes, Atkinson and Boore,

1995) is considerably larger, possibly reflecting the tectonic significance.

Stress parameter $\widetilde{\Delta\sigma}$ may not be equal to the average static stress drop $\Delta\sigma_s$ on the fault (Atkinson and Beresnev, 1998). In the literature, the apparent stress σ_a was considered as an estimate that is related with dynamic stress and rupture velocity (Madariaga, 1976; Boatwright, 1984b; Ji and Archuleta, 2020). We suspect that stress parameter $\widetilde{\Delta\sigma}$ is related with dynamic and rupture velocity as well. The inequality $\widetilde{\Delta\sigma} > \Delta\sigma_s$ has been noticed during the studies of large California and eastern North America earthquakes (e.g., Hanks and McGuire, 1981; Boore, 1983; Atkinson and Beresnev, 1998). This inequality may on average hold for $M_w > 5$ SCEs in tectonically active regions. For these earthquakes, the scaling relationship $M \sim \log(A) + 4$, in which A is in km^2, is generally applied (e.g., Leonard, 2010). This scaling relation suggests a $\Delta\sigma_s$ of 3 MPa. By analyzing the results of finite-fault slip models, Somerville *et al.* (1999) and Irikura and Miyake (2010) reported a mean $\Delta\sigma_s$ of 2.3 MPa. Both the results are smaller than the $\widetilde{\Delta\sigma}$ of 4.64 MPa (Baltay and Hanks, 2014). If $\widetilde{\Delta\sigma}$ of 4.64 MPa is equivalent with $\sigma_a \sim 1.1$ MPa and $\Delta\sigma_s \sim 3.0$ MPa, η_R^A of 0.7 would be suggested. The inequality $\widetilde{\Delta\sigma} > \Delta\sigma_s$ of SCEs, which still needs further confirmation, then suggests that the mean η_R^A of SCEs is ~50% larger than that of Brune's model (~0.466, Table 1). SCEs radiate, on average, more seismic energy than what is predicted by Brune's model, Madariaga's model, and K&S's model.

However, this interpretation has caveats. First, $\widetilde{\Delta\sigma}$ is constrained by the seismic radiation within a limited frequency band. The strong ground motion parameters such as PGA and PGV, used to constrain $\widetilde{\Delta\sigma}$ (Hanks and McGuire, 1981; Boore, 1983; Baltay and Hanks, 2014), are sensitive to band-limited seismic signals. Because of path attenuation, seismic signals with frequency above 8–10 Hz have negligible contributions to the strong ground motion parameters (Hanks and McGuire, 1981; Anderson and Hough, 1984; Baltay and Hanks, 2014). PGAs and PGVs in near-fault regions are also less sensitive to the relatively long period (<2 Hz) seismic signals (Atkinson and Silva, 2000). Using $\widetilde{\Delta\sigma}$ of 4.64 MPa, the corresponding corner frequency for **M** >5 earthquakes is less than 0.9 Hz. For such earthquakes, the predicted high-frequency acceleration source spectrum is essentially flat from 2 to 10 Hz with a spectral level $A_{hf} = [0.49\beta]^2 M_0^{1/3} \widetilde{\Delta\sigma}^{2/3}$ (β, M_0, and $\widetilde{\Delta\sigma}$ are in units of m/s, N · m, and Pascal, respectively). The success of Brune's model (which predicts no directivity) in engineering applications is consistent with the observations that rupture directivity effects during large earthquakes become negligible for seismic signals with frequency larger than 1.5 Hz (Somerville *et al.*, 1997). However, the dynamic cause of this lack of directivity effect in high frequency radiation is still under investigations (e.g., Bernard *et al.*, 1996; Gusev, 2013; Tsai and Hirth, 2020).

Second, Atkinson and Silva (2000) pointed out that despite its success in modeling high-frequency ground motions, a single corner frequency point source consistently overpredicts ground motions from moderate to large earthquakes at low-to-intermediate frequencies (~0.1 to 2 Hz) in California and elsewhere. A slight decrease of $\widetilde{\Delta\sigma}$ with magnitude for M_w 5.0–7.5 earthquakes was observed (Atkinson and Silva, 1997); this can be interpreted as a finite fault effect (Atkinson and Silva, 1997) or a consequence of the non-self-similar scaling fault length relation (Ji and Archuleta, 2022).

Third, the value of $\widetilde{\Delta\sigma}$ is related with the assumptions about site effects, geometric spreading, and earth attenuation (Boore, 1983; Baltay and Hanks, 2014). The uncertainty of $\widetilde{\Delta\sigma}$ reported in Cotton *et al.* (2013) was simply mapped from the uncertainty of attenuated ground motion observations through a scaling relationship. In contrast, σ_a is typically constrained by observations for which the effects of earth attenuation and geometric spreading factor were corrected (e.g., Ide *et al.*, 2003; Mayeda *et al.*, 2007). The assumptions about these effects used in earthquake seismology might not be same as what were used in engineering seismology. Because of the importance of $\widetilde{\Delta\sigma}$ in engineering seismology and σ_a in earthquake seismology, systematic investigations of $\Delta\sigma_{E_R}^{\mathrm{B}}$ and $\widetilde{\Delta\sigma}$ remain a high priority.

Relations among $\Delta\sigma_s$, $\Delta\sigma_{f_c}$, $\Delta\sigma_{E_R}$, and $\widetilde{\Delta\sigma}$

Aki (1967) proposed the self-similar earthquake model that has an omega-square source spectrum with corner frequency f_c and seismic moment M_0 satisfying $M_0 \propto f_c^{-3}$. Because of $\sigma_a \propto M_0 f_c^3$ (equation 8), Aki's scaling law leads to magnitude-independent apparent stress σ_a (Madariaga, 2011). By further assuming $f_c \propto 1/T_d$ (T_d is rupture duration), constant rupture velocity V_R, and $T_d \propto \tilde{L}/V_R$, Aki (1967) linked the corner frequency with fault length $\tilde{L}$ and claimed that the assumption of similarity implies a constant static stress drop $\Delta\sigma_s$ independent of source size. Aki's three assumptions were widely adopted in the late source scaling analyses (e.g., Kanamori and Anderson, 1975; Vallée, 2013). For the source spectral models summarized in Table 1, the relation between f_c and $\tilde{L}(= 2a, a$ is radius of the fault plane) depends on coefficient k. The difference in k suggests that this relation is nonunique even for an ideal radially propagating circular rupture with a constant V_R. Because the stress drop $\Delta\sigma_{f_c}$ is proportional to $\bar{f}_c^3/k^3$ (equation 5b), the relation between $\Delta\sigma_{f_c}$ and $\Delta\sigma_s$ is subject to cubed uncertainty from not only the measurement error of $\bar{f}_c$ but also the model uncertainty of k. The potential errors of $\bar{f}_c$ due to sampling bias, limits of integration, and the necessary radiation pattern and path effect corrections were discussed previously (see a recent review, Abercrombie, 2021). Natural earthquakes often have irregular fault planes, arbitrary hypocenter locations, and heterogeneous slip distributions. Consequently, k may be different for every earthquake. Even if we obtain a precise $\bar{f}_c$ measurement, $\Delta\sigma_{f_c}$ could be significantly different with $\Delta\sigma_s$, and the ratio of $\Delta\sigma_{f_c}$ and $\Delta\sigma_s$ is not a simple constant. The mean and standard deviation of such event-dependent k are then

critical and desired for further investigations. In similar, the relation between $\Delta\sigma_{f_c}$ and stress parameter $\widetilde{\Delta\sigma}$ also suffers from both the measurement error of $\bar{f}_c$ and the model uncertainty of k. $\widetilde{\Delta\sigma}$ may bear no relationship to real static stress drop $\Delta\sigma_s$ on the fault surface (Atkinson and Beresnev, 1998) but because of the way it was defined (Boore, 1983), $\widetilde{\Delta\sigma}$ scales with apparent stress σ_a. We notice that the k that is used to relate $\Delta\sigma_s$ with $\bar{f}_c$ cannot be directly applied for the prediction of σ_a.

It is of interest to summarize the relationship between $\Delta\sigma_{E_R}$ and $\Delta\sigma_{f_c}$. On one hand, $\Delta\sigma_{E_R}$, which is introduced in this study, is equal to $\Delta\sigma_{f_c}$ if the earthquake was well modeled by one of the corresponding spectral models, for example, the K&S model. The k^{E_R} of the three conventional source spectral models is close to the k of Brune's model (Table 1). On the other hand, if the observed source spectra cannot be precisely modeled with an omega-square Brune spectrum for every takeoff angle, $\bar{f}_c^{E_R}$ can be considerably different from $\bar{f}_c$ (e.g., $\bar{f}_c^{E_R} = 1.45\bar{f}_c$ for K&S model, Table 1). In such circumstances, even if one uses k^{E_R} and k for the same spectral model, $\Delta\sigma_{E_R}$ and $\Delta\sigma_{f_c}$ are expected to be different for earthquakes whose source spectra are better matched with spectral models that have more than one corner frequency (e.g., Brune, 1970; Gusev, 1983; Archuleta and Ji, 2016; Denolle and Shearer, 2016; Ji and Archuleta, 2020). Though the theoretical relationship between $\Delta\sigma_{E_R}$ and $\Delta\sigma_s$ is hard to define quantitatively, we find an empirically rough agreement between $\Delta\sigma_{E_R}$ and $\Delta\sigma_s$ exists for $M_w > 5.5$ earthquakes, and $\Delta\sigma_{E_R}$ is on average slightly larger for SCEs in tectonic regions. From a perspective of E_R conservation, $\widetilde{\Delta\sigma} = \Delta\sigma_{E_R}^B$ (Table 1). This theoretical consistency is useful if one attempts to investigate whether $\widetilde{\Delta\sigma}$ of moderate-to-large earthquakes, which is correlated with strong ground motion, can be predicted using the stress drop of small earthquakes (e.g., Hardebeck, 2020).

In the end, it is noteworthy that similar to $\Delta\sigma_{f_c}$, the measurements of seismic radiated energy E_R or apparent stress σ_a are also error prone, especially for small earthquakes (e.g., Ide and Beroza, 2001; Kanamori and Rivera, 2004; Baltay *et al.*, 2011; Abercrombie, 2021). Generally, the aforementioned sources of errors that contaminate $\bar{f}_c$ measurements (e.g., Abercrombie, 2021) will also affect $\Delta\sigma_{E_R}$ measurements. However, the quality of E_R measurements has been gradually improving with the advances in seismic observations and methodology (e.g., Mayeda and Walter, 1996; Boatwright *et al.*, 2002; Venkataraman *et al.*, 2002; Ide *et al.*, 2003; Abercrombie and Rice, 2005; Mayeda *et al.*, 2007; Baltay *et al.*, 2010; Walter *et al.*, 2017; Kanamori *et al.*, 2020).

CONCLUSIONS

Although the conventional source spectral models can lead to widely different estimates of static stress drop $\Delta\sigma_s$, they all predict that earthquakes radiate about half of the available strain energy to the surrounding medium. This suggests that the E_R-based stress drop, for example $\Delta\sigma_{E_R}$ (Snoke, 1987), is less model dependent. The relation $\Delta\sigma_{E_R}$ and $\Delta\sigma_s$ is sensitive to the apparent radiation efficiency η_R^A. Previous studies suggested that η_R^A of large SCEs varies within a relatively limited range around the predictions of the conventional source spectral models. Thus, on average, the E_R-based stress drop gives a reasonable approximation to $\Delta\sigma_s$.

Except for the Brune (1970) model, source spectral models were developed by constructing the relationship between the spherical mean corner frequency $\bar{f}_c$ and static stress drop $\Delta\sigma_s$ using the synthetic data generated by the dynamic or kinematic rupture models (e.g., Sato and Hirasawa, 1973; Madariaga, 1976; Kaneko and Shearer, 2014). Corner frequency and high-frequency fall-off rate change with the takeoff angle. Because of $(\bar{f}_c)^3 \le \overline{f_c^3}$, $\bar{f}_c$ cannot be used to make reliable forward predictions of ground motion or radiated seismic energy without additional corrections. From a perspective of conserving total radiated seismic energy, Brune's model is the only choice among the three conventional models for the forward prediction if one does not make the correction related with c_p.

We argue that the nearly constant stress parameter $\widetilde{\Delta\sigma}$ found in engineering seismology (e.g., Boore, 1983; Baltay and Hanks, 2014) is equivalent to having constant apparent stress σ_a in earthquake seismology (e.g., Ide and Beroza, 2001). For $M_w > 5.5$ SCEs, $\widetilde{\Delta\sigma}$ is roughly independent of magnitude and, on average, larger than $\Delta\sigma_s$. It is equivalent to saying that SCEs radiate, on average, more seismic energy than what is predicted from the three conventional dynamic crack models. Within the uncertainty, the spectral models for the SCEs in the active tectonic regions (Ancheta *et al.*, 2014), that is, AS00 (Atkinson and Silva, 2000), BH14 (Baltay and Hanks, 2014), and JA19 and JA19_2S (Ji and Archuleta, 2020), can be reconciled with $\sigma_a \sim 1.0$ MPa (Ide and Beroza, 2001; Baltay *et al.*, 2011; Kanamori *et al.*, 2020). This consistency, which needs further confirmation, is important. It suggests that the strong ground motion parameters collected in the studies of engineering seismology, such as PGAs and PGVs, are useful datasets to constrain the seismic radiated energy. The scatter of σ_a was substantially reduced if one considers seismic region, tectonic setting, and fault type (Choy *et al.*, 2006), which may also be used to reduce the scatter of $\widetilde{\Delta\sigma}$ in seismic hazard assessment.

DATA AND RESOURCES

All inferences were made through the analyses of the respective equations and literature sources as indicated. All calculations are done with open-source Julia language (https://julialang.org), and Figures are created with PyPlot (https://matplotlib.org/). All websites were last accessed in December 2021.

DECLARATION OF COMPETING INTERESTS

The authors acknowledge that there are no conflicts of interest recorded.

ACKNOWLEDGMENTS

The authors are grateful for the discussions with Steve Day and Lingling Ye. The authors thank Rachel Abercrombie and an anonymous reviewer for comments that improved the article. This study is supported by grants from the Southern California Earthquake Center (SCEC)—funded by National Science Foundation (NSF) cooperative Agreement Number EAR-0109624 and U.S. Geological Survey (USGS) cooperative Agreement Number 02HQAG0008. The authors received support from University of California, Santa Barbara (UCSB) matching grants to SCEC. All calculations were done with open-source Julia language, and Figures were created with Pyplot (https://matplotlib.org/, last accessed December 2021). This is SCEC contribution 11870.

REFERENCES

Abercrombie, R. E. (2021). Resolution and uncertainties in estimates of earthquake stress drop and energy release, *Phil. Trans. Roy. Soc. Lond. A* **379,** no. 2196, doi: 10.1098/rsta.2020.0131.

Abercrombie, R. E., and J. R. Rice (2005). Can observations of earthquake scaling constrain slip weakening? *Geophys. J. Int.* **162,** no. 2, 406–424, doi: 10.1111/j.1365-246X.2005.02579.x.

Abercrombie, R. E., D. T. Trugman, P. M. Shearer, X. W. Chen, J. W. Zhang, C. N. Pennington, J. L. Hardebeck, T. H. W. Goebel, and C. J. Ruhl (2021). Does earthquake stress drop increase with depth in the crust? *J. Geophys. Res.* **126,** no. 10, doi: 10.1029/2021JB022314.

Adams, M., J. L. Hao, and C. Ji (2019). Energy-based average stress drop and its uncertainty during the 2015 M-w 7.8 Nepal earthquake constrained by geodetic data and its implications to earthquake dynamics, *Geophys. J. Int.* **217,** no. 2, 784–797, doi: 10.1093/gji/ggz047.

Adams, M., C. Twardzik, and C. Ji (2017). Exploring the uncertainty range of coseismic stress drop estimations of large earthquakes using finite fault inversions, *Geophys. J. Int.* **208,** no. 1, 86–100, doi: 10.1093/gji/ggw374.

Aki, K. (1967). Scaling law of seismic spectrum, *J. Geophys. Res.* **72,** no. 4, 1217–1231, doi: 10.1029/JZ072i004p01217.

Aki, K. (1972). Earthquake mechanism, *Tectonophysics* **13,** nos. 1/4, 423–446.

Aki, K. (1984). Asperities, barriers, characteristic earthquakes and strong motion prediction, *J. Geophys. Res.* **89**, no. B7, 5867–5872, doi: 10.1029/JB089iB07p05867.

Allmann, B. P., and P. M. Shearer (2009). Global variations of stress drop for moderate to large earthquakes, *J. Geophys. Res.* **114,** no. B1, doi: 10.1029/2008jb005821.

Ancheta, T. D., R. B. Darragh, J. P. Stewart, E. Seyhan, W. J. Silva, B. S. J. Chiou, K. E. Wooddell, R. W. Graves, A. R. Kottke, D. M. Boore, *et al.* (2014). NGA-West2 database, *Earthq. Spectra,* **30,** no. 3, 989–1005, doi: 10.1193/070913EQS197M.

Anderson, J. G., and S. E. Hough (1984). A model for the shape of the Fourier amplitude spectrum of acceleration at high-frequencies, *Bull. Seismol. Soc. Am.* **74,** no. 5, 1969–1993.

Andrews, D. J. (1986). Objective determination of source parameters and similarity of earthquakes of different size, in *Earthquake Source Mechanics*, Geophysical Monograph Series, S. Das, J. Boatwright, and C. H. Scholz (Editors), Vol. 37, American Geophysical Union, Washington DC, 259–267.

Archuleta, R. J., and C. Ji (2016). Moment rate scaling for earthquakes 3.3M5.3 with implications for stress drop, *Geophys. Res. Lett.* **43,** no. 23, 12,004–12,011.

Asano, K., and T. Iwata (2011). Characterization of stress drops on asperities estimated from the heterogeneous kinematic slip model for strong motion prediction for inland crustal earthquakes in Japan, *Pure Appl. Geophys.* **168,** nos. 1/2, 105–116, doi: 10.1007/s00024-010-0116-y.

Atkinson, G. M., and I. Beresnev (1998). Don't call it stress drop, *Seismol. Res. Lett.* **68,** no. 1, 3–4.

Atkinson, G. M., and D. M. Boore (1995). Ground-motion relations for eastern north-America, *Bull. Seismol. Soc. Am.* **85,** no. 1, 17–30.

Atkinson, G. M., and W. Silva (1997). An empirical study of earthquake source spectra for California earthquakes, *Bull. Seismol. Soc. Am.* **87,** no. 1, 97–113.

Atkinson, G. M., and W. Silva (2000). Stochastic modeling of California ground motions, *Bull. Seismol. Soc. Am.* **90,** no. 2, 255–274, doi: 10.1785/0119990064.

Baltay, A., and T. C. Hanks (2014). Understanding the magnitude dependence of PGA and PGV in NGA-West 2 data, *Bull. Seismol. Soc. Am.* **104,** no. 6, 2851–2865.

Baltay, A., G. Prieto, and G. C. Beroza (2010). Radiated seismic energy from coda measurements and no scaling in apparent stress with seismic moment, *J. Geophys. Res.* **115**, doi: 10.1029/2009jb006736.

Baltay, A., S. Ide, G. Prieto, and G. Beroza (2011). Variability in earthquake stress drop and apparent stress, *Geophys. Res. Lett.* **38,** doi: 10.1029/2011gl046698.

Beeler, N. M., T. F. Wong, and S. H. Hickman (2003). On the expected relationships among apparent stress, static stress drop, effective shear fracture energy, and efficiency, *Bull. Seismol. Soc. Am.* **93,** no. 3, 1381–1389, doi: 10.1785/0120020162.

Bernard, P., A. Herrero, and C. Berge (1996). Modeling directivity of heterogeneous earthquake ruptures, *Bull. Seismol. Soc. Am.* **86,** no. 4, 1149–1160.

Beroza, G. C., and T. Mikumo (1996). Short slip duration in dynamic rupture in the presence of heterogeneous fault properties, *J. Geophys. Res.* **101,** no. B10, 22,449–22,460, doi: 10.1029/96jb02291.

Boatwright, J. (1984a). The effect of rupture complexity on estimates of source size, *J. Geophys. Res.* **89,** no. B2, 1132–1146, doi: 10.1029/JB089iB02p01132.

Boatwright, J. (1984b). Seismic estimates of stress release, *J. Geophys. Res.* **89,** no. B8, 6961–6968, doi: 10.1029/JB089iB08p06961.

Boatwright, J. (1988). The seismic radiation from composite models of faulting, *Bull. Seismol. Soc. Am.* **78,** no. 2, 489–508.

Boatwright, J., G. L. Choy, and L. C. Seekins (2002). Regional estimates of radiated seismic energy, *Bull. Seismol. Soc. Am.* **92,** no. 4, 1241–1255, doi: 10.1785/0120000932.

Boore, D. (1983). Stochastic simulation of high-frequency ground motions based on seismological models of the radiated spectra, *Bull. Seismol. Soc. Am.* **73,** no. 6, 1865–1894.

Boore, D. M. (2003). Simulation of ground motion using the stochastic method, *Pure Appl. Geophys.* **160,** nos. 3/4, 635–676, doi: 10.1007/Pl00012553.

Boore, D., C. Di Alessandro, and N. A. Abrahamson (2014). A generalization of the double-corner-frequency source spectral model and its use in the SCEC BBP validation exercise, *Bull. Seismol. Soc. Am.* **104,** no. 5, 2387–2398, doi: 10.1785/0120140138.

Bouchon, M. (1997). The state of stress on some faults of the San Andreas system as inferred from near-field strong motion data, *J. Geophys. Res.* **102,** no. B6, 11,731–11,744, doi: 10.1029/97jb00623.

Brown, L., K. Wang, and T. Sun (2015). Static stress drop in the Mw 9 Tohoku-Oki earthquake: Heterogeneous distribution and low average value, *Geophys. Res. Lett.* **42,** no. 24, 10,595–10,600, doi: 10.1002/2015gl066361.

Brune, J. N. (1970). Tectonic stress and spectra of seismic shear waves from earthquakes, *J. Geophys. Res.* **75,** no. 26, 4997–5009.

Brune, J. N. (1971). Correction, *J. Geophys. Res.* **76,** no. 20, 5002–5002.

Choy, G. L., and J. L. Boatwright (1995). Global patterns of radiated seismic energy and apparent stress, *J. Geophys. Res.* **100,** no. B9, 18,205–18,228, doi: 10.1029/95jb01969.

Choy, G. L., A. McGarr, S. H. Kirby, and J. Boatwright (2006). An overview of the global variability in radiated energy and apparent stress, in *Earthquakes: Radiated Energy and the Physics of Faulting*, R. E. Abercrombie, A. McGarr, H. Kanamori, and G. Di Toro (Editors), American Geophysical Union, Washington DC, 43–57.

Convers, J. A., and A. V. Newman (2011). Global evaluation of large earthquake energy from 1997 through mid-2010, *J. Geophys. Res.* **116,** doi: 10.1029/2010jb007928.

Cotton, F., R. Archuleta, and M. Causse (2013). What is sigma of the stress drop? *Seismol. Res. Lett.* **84,** no. 1, 42–48, doi: 10.1785/0220120087.

Day, S. M. (1982). 3-dimensional finite-difference simulation of fault dynamics—Rectangular faults with fixed rupture velocity, *Bull. Seismol. Soc. Am.* **72,** no. 3, 705–727.

Denolle, M. A., and P. M. Shearer (2016). New perspectives on self-similarity for shallow thrust earthquakes, *J. Geophys. Res.* **121,** no. 9, 6533–6565, doi: 10.1002/2016jb013105.

Dreger, D., R. M. Nadeau, and A. Chung (2007). Repeating earthquake finite source models: Strong asperities revealed on the San Andreas fault, *Geophys. Res. Lett.* **34,** no. 23, doi: 10.1029/2007gl031353.

Eshelby, J. D. (1957). The determination of the elastic field of an ellipsoidal inclusion, and related problems, *Proc. Roy. Soc. Lond. Ser. A* **241,** no. 1226, 376–396, doi: 10.1098/rspa.1957.0133.

Graves, R. W., and A. Pitarka (2010). Broadband ground-motion simulation using a hybrid approach, *Bull. Seismol. Soc. Am.* **100,** no. 5, 2095–2123, doi: 10.1785/0120100057.

Gusev, A. A. (1983). Descriptive statistical-model of earthquake source radiation and its application to an estimation of short-period strong motion, *Geophys. J. Roy. Astr. Soc.* **74,** no. 3, 787–808.

Gusev, A. A. (2013). High-frequency radiation from an earthquake fault: A review and a hypothesis of fractal rupture front geometry, *Pure Appl. Geophys.* **170,** no. 1–2, 65–93, doi: 10.1007/s00024-012-0455-y.

Hanks, T. C. (2002). A bilinear source-scaling model for M-log A observations of continental earthquakes, *Bull. Seismol. Soc. Am.* **92,** no. 5, 1841–1846, doi: 10.1785/0120010148.

Hanks, T. C., and W. H. Bakun (2008). M-log A observations for recent large earthquakes, *Bull. Seismol. Soc. Am.* **98,** no. 1, 490–494, doi: 10.1785/0120070174.

Hanks, T. C., and R. K. McGuire (1981). The character of high-frequency strong ground motion, *Bull. Seismol. Soc. Am.* **71,** no. 6, 2071–2095.

Hardebeck, J. L. (2020). Are the stress drops of small earthquakes good predictors of the stress drops of moderate-to-large earthquakes? *J. Geophys. Res.* **125,** no. 3. doi: 10.1029/2019jb018831.

Heaton, T. H. (1990). Evidence for and implications of self-healing pulses of slip in earthquake rupture, *Phys. Earth Planet. In.* **64,** no. 1, 1–20, doi: 10.1016/0031-9201(90)90002-F.

Husseini, M. I., and M. J. Randall (1976). Rupture velocity and radiation efficiency, *Bull. Seismol. Soc. Am.* **66,** no. 4, 1173–1187.

Ide, S., and G. C. Beroza (2001). Does apparent stress vary with earthquake size? *Geophys. Res. Lett.* **28,** no. 17, 3349–3352, doi: 10.1029/2001gl013106.

Ide, S., G. C. Beroza, S. G. Prejean, and W. L. Ellsworth (2003). Apparent break in earthquake scaling due to path and site effects on deep borehole recordings, *J. Geophys. Res.* **108,** no. B5, doi: 10.1029/2001jb001617.

Irikura, K., and H. Miyake (2010). Recipe for predicting strong ground motion from crustal earthquake scenarios, *Pure Appl. Geophys.* **168,** nos. 1/2, 85–104, doi: 10.1007/s00024-010-0150-9.

Ji, C., and R. J. Archuleta (2020). Two empirical double-corner-frequency source spectra and their physical implications, *Bull. Seismol. Soc. Am.* doi: 10.1785/0120200238.

Ji, C., and R. J. Archuleta (2021). Two empirical double-corner-frequency source spectra and their physical implications, *Bull. Seismol. Soc. Am.* **111,** no. 2, 737–761, doi: 10.1785/0120200238.

Ji, C., and R. J. Archuleta (2022). A source physics interpretation of nonself-similar double-corner-frequency source spectral model JA19_2S, *Seismol. Res. Lett.* **93,** no. 2A, 777–786, doi: 10.1785/0220210098.

Kanamori, H. (1978). Quantification of great earthquakes, *Tectonophysics* **49,** nos. 3/4, 207–212. doi: 10.1016/0040-1951(78)90179-8.

Kanamori, H. (1994). Mechanics of earthquakes, *Annu. Rev. Earth Planet. Sci.* **22,** 207–237, doi: 10.1146/annurev.ea22.050194.001231.

Kanamori, H., and D. L. Anderson (1975). Theoretical basis of some empirical relations in seismology, *Bull. Seismol. Soc. Am.* **65,** no. 5, 1073–1095.

Kanamori, H., and E. E. Brodsky (2004). The physics of earthquakes, *Rept. Prog. Phys.* **67,** no. 8, 1429–1496, doi: 10.1088/0034-4885/67/8/r03.

Kanamori, H., and L. Rivera (2004). Static and dynamic scaling relations for earthquakes and their implications for rupture speed and stress drop, *Bull. Seismol. Soc. Am.* **94,** no. 1, 314–319.

Kanamori, H., and L. Rivera (2006). Energy partitioning during an earthquake, in *Earthquakes: Radiated Energy and the Physics of Faulting*, R. E. Abercrombie, A. McGarr, H. Kanamori, and G. Di Toro (Editors), American Geophysical Union, Washington DC, 3–13.

Kanamori, H., Z. E. Ross, and L. Rivera (2020). Estimation of radiated energy using the KiK-net downhole records—Old method for modern data, *Geophys. J. Int.* **221,** no. 2, 1029–1042, doi: 10.1093/gji/ggaa040.

Kaneko, Y., and P. M. Shearer (2014). Seismic source spectra and estimated stress drop derived from cohesive-zone models of circular subshear rupture, *Geophys. J. Int.* **197,** no. 2, 1002–1015, doi: 10.1093/gji/ggu030.

Kaneko, Y., and P. M. Shearer (2015). Variability of seismic source spectra, estimated stress drop, and radiated energy, derived from cohesive-zone models of symmetrical and asymmetrical circular and elliptical ruptures, *J. Geophys. Res.* **120,** no. 2, 1053–1079, doi: 10.1002/2014jb011642.

Kikuchi, M., and Y. Fukao (1988). Seismic-wave energy inferred from long-period body wave inversion, *Bull. Seismol. Soc. Am.* **78,** no. 5, 1707–1724.

Lambert, V., N. Lapusta, and S. Perry (2021). Propagation of large earthquakes as self-healing pulses or mild cracks, *Nature* **591,** no. 7849, doi: 10.1038/s41586-021-03248-1.

Lay, T., H. Kanamori, and L. Ruff (1982). The asperity model and the nature of large subduction zone earthquakes, *Earthq. Pred. Res.* **1,** no. 1, 3–71.

Leonard, M. (2010). Earthquake fault scaling: Self-consistent relating of rupture length, width, average displacement, and moment release, *Bull. Seismol. Soc. Am.* **100,** no. 5A, 1971–1988, doi: 10.1785/0120090189.

Madariaga, R. (1976). Dynamics of an expanding circular fault, *Bull. Seismol. Soc. Am.* **66,** no. 3, 639–666.

Madariaga, R. (2011). Earthquake scaling laws, in *Extreme Environmental Events: Complexity in Forecasting and Early Warning*, R. A. Meyers (Editor), Springer, New York, 364–383.

Mai, P. M., and G. C. Beroza (2002). A spatial random field model to characterize complexity in earthquake slip, *J. Geophys. Res.* **107,** no. B11, doi: 10.1029/2001jb000588.

Mayeda, K., and W. R. Walter (1996). Moment, energy, stress drop, and source spectra of western United States earthquakes from regional coda envelopes, *J. Geophys. Res.* **101,** no. B5, 11,195–11,208, doi: 10.1029/96jb00112.

Mayeda, K., L. Malagnini, and W. R. Walter (2007). A new spectral ratio method using narrow band coda envelopes: Evidence for non-self-similarity in the Hector Mine sequence, *Geophys. Res. Lett.* **34,** no. 11, doi: 10.1029/2007gl030041.

McGuire, J. J., L. Zhao, and T. H. Jordan (2002). Predominance of unilateral rupture for a global catalog of large earthquakes, *Bull. Seismol. Soc. Am.* **92,** no. 8, 3309–3317, doi: 10.1785/0120010293.

Murotani, S., S. Matsushima, T. Azuma, K. Irikura, and S. Kitagawa (2015). Scaling relations of source parameters of earthquakes occurring on inland crustal mega-fault systems, *Pure Appl. Geophys.* **172,** no. 5, 1371–1381, doi: 10.1007/s00024-014-1010-9.

Noda, H., N. Lapusta, and H. Kanamori (2013). Comparison of average stress drop measures for ruptures with heterogeneous stress change and implications for earthquake physics, *Geophys. J. Int.* **193,** no. 3, 1691–1712, doi: 10.1093/gji/ggt074.

Oth, A., D. Bindi, S. Parolai, and D. Di Giacomo (2010). Earthquake scaling characteristics and the scale-(in)dependence of seismic energy-to-moment ratio: Insights from KiK-net data in Japan, *Geophys. Res. Lett.* **37,** no. 19, doi: 10.1029/2010gl044572.

Prieto, G. A., P. M. Shearer, F. L. Vernon, and D. Kilb (2004). Earthquake source scaling and self-similarity estimation from stacking P and S spectra, *J. Geophys. Res.* **109,** no. B8, doi: 10.1029/2004jb003084.

Ripperger, J., and P. M. Mai (2004). Fast computation of static stress changes on 2D faults from final slip distributions, *Geophys. Res. Lett.* **31,** no. 18, doi: 10.1029/2004gl020594.

Sato, T., and T. Hirasawa (1973). Body wave spectra from propagating shear cracks, *J. Phys. Earth* **21,** no. 4, 415–431, doi:10.4294/jpe1952.21.415.

Savage, J. C., and M. D. Wood (1971). Relation between apparent stress and stress drop, *Bull. Seismol. Soc. Am.* **61,** no. 5, 1381–1388.

Shao, G. F., C. Ji, and E. Hauksson (2012). Rupture process and energy budget of the 29 July 2008 M-w 5.4 Chino Hills, California, earthquake, *J. Geophys. Res.* **117,** doi: 10.1029/2011jb008856.

Shearer, P. M., and R. E. Abercrombie (2021). Calibrating spectral decomposition of local earthquakes using borehole seismic records-results for the 1992 big bear aftershocks in southern California, *J. Geophys. Res.* **126,** no. 3, doi: 10.1029/2020JB020561.

Shearer, P. M., G. A. Prieto, and E. Hauksson (2006). Comprehensive analysis of earthquake source spectra in southern California, *J. Geophys. Res.* **111,** no. B6, doi: 10.1029/2005jb003979.

Shearer, P. M., R. E. Abercrombie, D. T. Trugman, and W. Wang (2019). Comparing EGF methods for estimating corner frequency and stress drop from P wave spectra, *J. Geophys. Res.* **124,** no. 4, 3966–3986, doi: 10.1029/2018jb016957.

Singh, S. K., and M. Ordaz (1994). Seismic energy-release in Mexican subduction zone earthquakes, *Bull. Seismol. Soc. Am.* **84,** no. 5, 1533–1550.

Snoke, J. A. (1987). Stable determination of (Brune) stress drops, *Bull. Seismol. Soc. Am.* **77,** no. 2, 530–538.

Somerville, P., K. Irikura, R. Graves, S. Sawada, D. Wald, N. Abrahamson, Y. Iwasaki, T. Kagawa, N. Smith, and A. Kowada (1999). Characterizing crustal earthquake slip models for the prediction of strong ground motion, *Seismol. Res. Lett.* **70,** no. 1, 59–80, doi: 10.1785/gssrl.70.1.59.

Somerville, P. G., N. F. Smith, R. W. Graves, and N. A. Abrahamson (1997). Modification of empirical strong ground motion attenuation relations to include the amplitude and duration effects of rupture directivity, *Seismol. Res. Lett.* **68,** no. 1, 199–222, doi: 10.1785/gssrl.68.1.199.

Tsai, V. C., and G. Hirth (2020). Elastic impact consequences for high?frequency earthquake ground motion, *Geophys. Res. Lett.* **47,** no. 5, doi: 10.1029/2019gl086302.

Vallée, M. (2013). Source time function properties indicate a strain drop independent of earthquake depth and magnitude, *Nat. Commun.* **4,** doi: 10.1038/ncomms3606.

Venkataraman, A., and H. Kanamori (2004). Observational constraints on the fracture energy of subduction zone earthquakes, *J. Geophys. Res.* **109,** no. B5, doi: 10.1029/2003jb002549.

Venkataraman, A., L. Rivera, and H. Kanamori (2002). Radiated energy from the 16 October 1999 Hector Mine earthquake: Regional and teleseismic estimates, *Bull. Seismol. Soc. Am.* **92,** no. 4, 1256–1265, doi: 10.1785/0120000929.

Walter, W. R., S. H. Yoo, K. Mayeda, and R. Gök (2017). Earthquake stress via event ratio levels: Application to the 2011 and 2016 Oklahoma seismic sequences, *Geophys. Res. Lett.* **44,** no. 7, 3147–3155, doi: 10.1002/2016gl072348.

Wang, Y., and S. M. Day (2017). Seismic source spectral properties of crack-like and pulse-like modes of dynamic rupture, *J. Geophys. Res.* **122,** no. 8, 6657–6684, doi: 10.1002/2017jb014454.

Wells, D. L., and K. J. Coppersmith (1994). New empirical relationships among magnitude, rupture length, rupture width, rupture area, and surface displacement, *Bull. Seismol. Soc. Am.* **84,** no. 4, 974–1002.

Wyss, M., and J. N. Brune (1968). Seismic moment stress and source dimensions for earthquakes in California-Nevada region, *J. Geophys. Res.* **73,** no. 14, doi: 10.1029/JB073i014p04681.

Ye, L. L., T. Lay, H. Kanamori, and L. Rivera (2016). Rupture characteristics of major and great (M-w >= 7.0) megathrust earthquakes from 1990 to 2015: 1. Source parameter scaling relationships, *J. Geophys. Res.* **121,** no. 2, 826–844, doi: 10.1002/2015jb012426.

APPENDIX

Seismic radiation efficiency of Maradiaga's model (Madariaga, 1976)

Madariaga (1976) derived the relationship between the apparent stress σ_a and effective (dynamic) stress drop τ_e for his model:

$$\sigma_a = \frac{1}{2}\tau_e\left[2 - \Delta\sigma^{'} - \frac{g(V_R)}{D}\right]. \quad \text{(A1)}$$

Here, $g(V_R)$ represents the contribution of the fracture energy, which is a function of rupture velocity; D is the slip at the center of the fault, and $\Delta\sigma^{'}$ denotes the ratio of static stress drop $\Delta\sigma_s$ and τ_e (Madariaga, 1976). $g(V_R)$ and $\Delta\sigma^{'}$ are sensitive to the rupture velocity. Madariaga (1976) reported the values of these two functions for two rupture velocities when $V_R = 0.9\beta$, $\Delta\sigma^{'} = \Delta\sigma_s/\tau_e = 1.2$, and $g(V_R) = 0.21$. Without overshoot the static crack solution (Eshelby, 1957) of fault slip at the center is $\frac{24}{7\pi} \sim 1.09$ (nondimensional, Madariaga, 1976). Because of overshoot, D is $(1.31 - \Delta\sigma^{'})$ times larger than the static solution. Using these values in equation (A1), $\sigma_a \cong 0.267\Delta\sigma_s$. Assuming $\Delta\sigma_s^E = \Delta\sigma_s$, we find $\eta_R \sim 0.533$. With $V_R = 0.6\beta$, $\Delta\sigma^{'} = 1.15$, and $g(V_R) = 0.72$, giving $\sigma_a \cong 0.120\Delta\sigma_s$ and $\eta_R \cong 0.240$. For both the rupture velocities, the estimates of η_R are larger than the estimates of Kaneko and Shearer (2015) by 11%–20%. These differences could be explained by the differences in $\Delta\sigma^{'}$; Kaneko and Shearer (2015) have $\Delta\sigma^{'}$ equal to 1.26 for $V_R = 0.9\beta$ and 1.21 for $V_R = 0.6\beta$.

Manuscript received 15 December 2021
Published online 17 June 2022